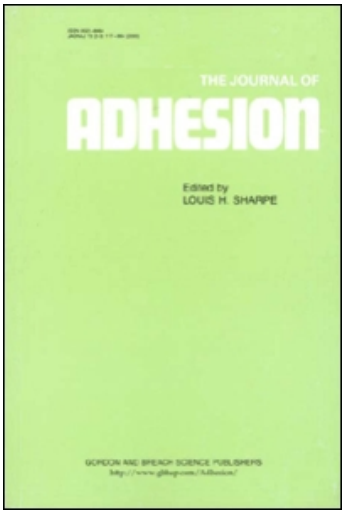

The Journal of Adhesion
Publication details, including instructions for authors and subscription information:
http://www.informaworld.com/smpp/title~content=t713453635

DLVO AND NON-DLVO FORCES IN THIN LIQUID FILMS FROM RHAMNOLIPIDS

R. Cohen[a]; D. Exerowa[a]; I. Pigov[a]; R. Heckmann[b]; S. Lang[b]
[a] Institute of Physical Chemistry, Bulgarian Academy of Sciences, Sofia, Bulgaria [b] Department of Biochemistry and Biotechnology, Technical University, Braunschweig, Germany

Online publication date: 10 August 2010

To cite this Article Cohen, R. , Exerowa, D. , Pigov, I. , Heckmann, R. and Lang, S.(2004) 'DLVO AND NON-DLVO FORCES IN THIN LIQUID FILMS FROM RHAMNOLIPIDS', The Journal of Adhesion, 80: 10, 875 — 894
To link to this Article: DOI: 10.1080/00218460490508580
URL: http://dx.doi.org/10.1080/00218460490508580

The Journal of Adhesion, 80: 875–894, 2004

ISSN: 0021-8464 print/1545-5823 online
DOI: 10.1080/00218460490508580

Taylor & Francis
Taylor & Francis Group

DLVO AND NON-DLVO FORCES IN THIN LIQUID FILMS FROM RHAMNOLIPIDS

R. Cohen
D. Exerowa
I. Pigov
Institute of Physical Chemistry, Bulgarian Academy of Sciences, Sofia, Bulgaria

R. Heckmann
S. Lang
Department of Biochemistry and Biotechnology, Technical University, Braunschweig, Germany

Microscopic foam films ($r = 100\,\mu m$) stabilized with a single rhamnolipid with a well-known structure (α-L-rhamnopyranosyl-β-hydroxydecanoyl-β-hydroxydecanoate (R1)) are investigated, and the obtained results are compared with results obtained from studies of foam films formed from solutions of rhamnolipid mixtures. The studies are carried out employing the Scheludko-Exerowa microinterferometric method. The dependence of foam film thickness on the electrolyte concentration (C_{el}) of the solution is monitored, and formation of common films (CF), common black films (CBF) and Newton black films (NBF) is found. The continuous CBF-to-NBF transition is considered as evidence of the action of repulsive forces that are not described by the classic Derjaguin–Landau–Verwey–Overbeek (DLVO) theory of colloid stability. These non-DLVO repulsive forces lead to an additional positive component of the disjoining pressure. To understand better the surface forces operating in the rhamnolipid foam films, direct measurements of the disjoining pressure/film thickness ($\Pi(h)$) isotherms are carried out employing the thin liquid film–pressure balance technique. The comparison of the obtained experimental $\Pi(h)$ isotherm for CF ($C_{el} = 10^{-3}$ mol dm^{-3} NaCl) to the DLVO theoretical predictions yields a diffuse electric layer potential of $\sim 5\,mV$ and surface

Received 29 January 2004; in final form 3 May 2004.

The authors are grateful to Mr. Ts. Mihailov, Institute of Inorganic Chemistry, Bulgarian Academy of Sciences, for his help in obtaining the simplified model of R1.

One of a collection of papers honoring A. W. Neumann, the recipient in February 2004 of *The Adhesion Society Award for Excellence in Adhesion Science, Sponsored by 3M*.

Address correspondence to Dotchi Exerowa, Institute of Physical Chemistry, Bulgarian Academy of Sciences, Acad. G. Bonchev Str., bl. 11, Sofia 1113, Bulgaria. E-mail: exerowa@ipchp.ipc.bas.bg

charge density of $\sim 50\,mC\,m^{-2}$ at the film solution–air interfaces. The deviation of the experimental curve from the theoretical one found for films thinner than about 40 nm evidences the action of non-DLVO surface forces. The experimental steplike $\Pi(h)$ isotherms obtained for the CBF ($C_{el} = 0.15\,mol\,dm^{-3}$ NaCl) are considered to result from an aggregation process, leading to the formation of lamellar structures in the foam film. The obtained results show that the surface forces operative in rhamnolipid foam films are determined not only by the structure and organization of the adsorbed layers but also by the molecular state of the bulk solution.

Keywords: Rhamnolipid foam films; DLVO surface forces; Non-DLVO surface forces; Stepwise isotherm; Diffuse electric layer potential; Surface charge density

INTRODUCTION

Thin liquid films have long been used for modeling interactions in disperse systems such as foams, emulsions, and suspensions [1–7]. The structure of the thin liquid films comprising large interfaces separated by a thin liquid core determines their different thermodynamic and kinetic properties compared with the bulk phase. The classic Derjaguin–Landau–Verwey–Overbeek (DLVO) theory of colloid stability [2, 6, 8] describes film stability as interplay between long-range electrostatic interactions and molecular van der Waals forces. In the case of symmetrical thin liquid films formed between the same adjacent phases (*e.g.*, foam films, emulsion films, and films formed between two solid surfaces) the electrostatic interactions are always positive because they cause repulsion of the film interfaces, while the attractive van der Waals interactions are negative. Detailed studies of thin liquid films during the last decades of the past century have also demonstrated the existence of other types of surface forces, *e.g.*, structural (or hydration) and steric forces, that are operative in certain types of thin liquid films [2, 6, 7, 9–14].

The phase boundaries of thin liquid films that are gaseous in the case of foam films, liquid in the case of emulsion films, or solid, determine to a great extent the surface forces operating in them. Thin liquid films can also form between different adjacent phases. Such are the films formed on a solid substrate, also called *wetting films*. Recent parallel investigations of symmetric foam and asymmetric wetting films formed from aqueous solutions of an ionic surfactant [15] and block copolymers [16] with NaCl as a background electrolyte demonstrate the role of electrostatic and steric forces for their stability. Such a comparison between foam and wetting films is very convenient when both types of films have the same solution–air interfaces

because it allows use of the results obtained from studies of the foam film with regard to the wetting film behavior.

The free liquid (foam) films have been the objects of numerous studies due to the simplicity of their formation, their geometrically well-defined surfaces, and last, but not least, because their precise experimental methods allow accurate measurement of various film parameters [1, 3–5, 7 and references therein]. The comparison of the obtained experimental results with the classic and contemporary theories of surface forces provide a way of understanding the reasons for formation and stability of films stabilized with various synthetic as well as natural, surfactants (biosurfactants) [7, 17–20]. Such natural surfactants (or biosurfactants) are the rhamnolipid-type biosurfactants that are synthesized by micro-organisms during their growth on hydrocarbon substrates. Similar to synthetic surfactants, these biosurfactants can be employed in various technical systems—as emulsifiers, as dispersants, to modify surfaces *etc*. [21–25]. The advantages of rhamnolipid biosurfactants over their synthetic counterparts are their biodegrability, low toxicity, and stability in a wide range of temperatures and pH. Because there are good prospects for the use of rhamnolipids as substitutes for commonly used synthetic surfactants of petrochemical origin, the study of their surface properties can be of interest for various practical purposes. The efficiency and effectiveness of these compounds are conventionally determined by their ability to reduce the surface tension of aqueous solutions and the interfacial tension of water–oil systems [23–28]. Such studies provide information on the adsorption and interfacial properties of different rhamnolipid species. Here, the foam film model offers unique possibilities for investigating the interaction forces between two solution–air interfaces through a thin liquid core.

Recent studies of surface forces in horizontal microscopic foam films (radius $\sim$100 μm) formed from aqueous solutions of a mixture of two rhamnolipid-type microbial surfactants show formation of common (CF), common block (CBF), or Newton black films (NBF), depending on the electrolyte concentration of the solution [29]. While CF are comparatively "thick" films, appearing white to gray in reflected light, the black films are so thin that they virtually reflect no light. The common black films (CBF) comprise a water core between the adsorbed layers at its air–solution interfaces while the structure of the thinnest NBF can be described as two monolayers of the surface active substance adsorbed on each other [7, 30]. The experimental studies [29] show that while DLVO surface forces determine the stability of the common films, non-DLVO surface forces leading to additional repulsive interactions become operative in CBF and NBF. These non-DLVO forces are

attributed to the complex structure of the strongly hydrophilic head groups of the rhamnolipid molecules and to the specificity of the organization of the adsorbed rhamnolipid ions with different head groups at the solution–air interfaces of the film.

In order to get further insight into the nature of surface forces operative in rhamnolipid foam films, it is important to investigate films formed not only of aqueous solutions of rhamnolipid mixtures but also of a single rhamnolipid with a well-known structure. That is why the objective of the present work is to investigate experimentally the surface forces in foam films stabilized with the rhamnolipid R1 (α-L-rhamnopyranosyl-β-hydroxydecanoyl-β-hydroxydecanoate). Such a study is of special importance for the understanding of the characteristic behavior of rhamnolipids at the solution–air interface.

EXPERIMENTAL

Materials

The foam films were obtained from solutions of the rhamnolipid R1 (α-L-rhamnopyranosyl-β-hydroxydecanoyl-β-hydroxydecanoate) with a single rhamnose group and molecular mass of 504. Figure 1 shows the chemical structure and a simplified model of R1 derived from PM3 method. Rhamnolipids are usually produced by *pseudomonas aeruginosa* micro-organisms as a mixture of two or four species [31]. In these lipids, the hydroxyl group of one of the fatty acids is linked by a glycosidic bond with the rhamnose saccharide or disaccharide and by an ester bond with the hydroxyl group of the second acid. For preparation of single compounds, at first 2 ml of the aqueous industrial sample 1.2 (Jeneil Biosurfactant Company, Saukville, WI, USA) was freeze-dried, giving 470 mg of water-free material. This rhamnolipid mixture, mainly consisting of the components R1 (one rhamnose unit, two decanoic acid units) and R2 (two rhamnoses, two decanoic acids), was dissolved in 3 ml of chloroform/methanol/water (65/15/2; v/v/v) and afterwards was separated by using medium-pressure liquid chromatography (MPLC). MPLC equipment was composed of a Lobar column, size B, LiChroprep® Si 60, 40–63 μm (Merck, Darmstadt, Germany), and a chromatography pump B 688 (Büchi, Konstanz, Germany). Chromatography was performed with chloroform/methanol/water (65/15/2, v/v/v) as the mobile phase at a pressure of 3 bar and a flow rate of 1 ml/min. The eluate was fractionized using the Pharmacia LKB Frac-100 collector (Pharmacia LKB, Freiburg, Germany). The purification of rhamnolipids was monitored off-line by thin layer chromatography (TLC). TLC was carried out on

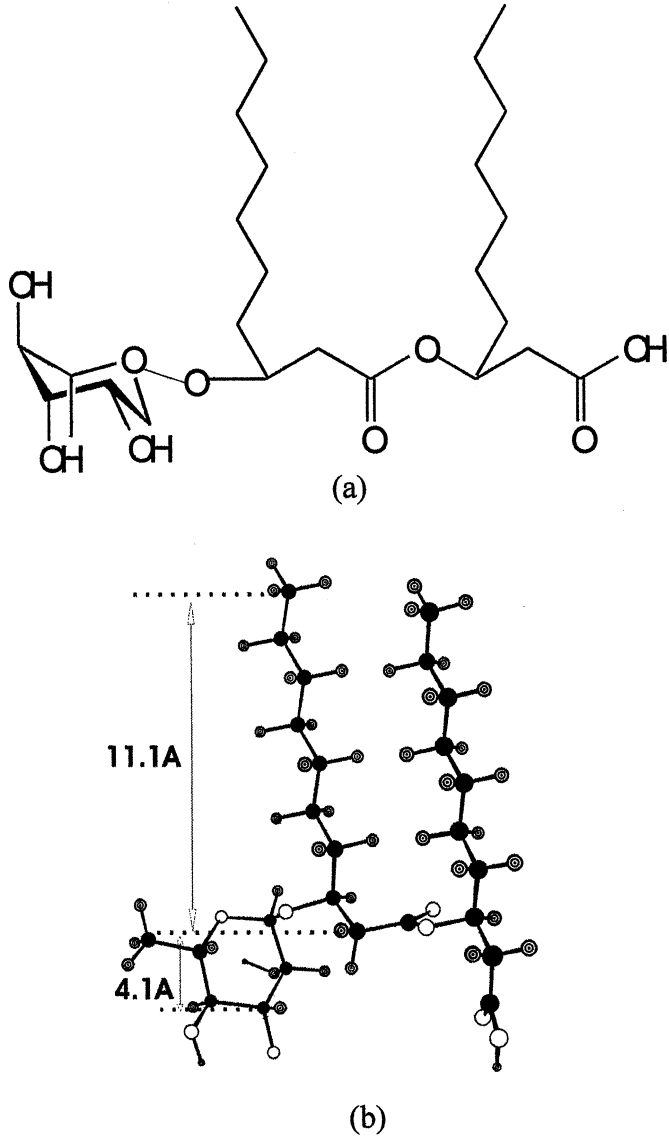

FIGURE 1 Chemical structure and simplified model of R1 derived from the MP3 method.

Si gel 60 plates as stationary phase with the same solvent system that was used for MPLC and with anisaldehyde/sulfuric acid reagent for detection of carbohydrate-positive compounds. To facilitate the

identification of R1 and R2, additionally the two corresponding rhamnolipids from *Pseudomonas* spec. DSM 2874 were used for comparison [32]. Based on those R_F values, the MPLC fractions containing the desired products were separately pooled, the solvents evaporated and subsequently the residual water freeze-dried. Finally, 70 mg of R1 and 150 mg of R2 were isolated.

To obtain a stock solution with a concentration, C_s, of 10^{-3} mol dm^3 R1, we added water to the isolated dry substance, vortexed the mixture for several minutes and heated it to 60–70°C to obtain a homogeneous suspension. After cooling we neutralized the suspension with dry NaOH at a 1:1 ratio and put it in a bath-type sonificator for 1 h.

Rhamnolipid solutions with a constant concentration of 5×10^{-4} mol dm^{-3} were prepared the day of investigation from the stock solution. This C_s was found as a result of an investigation of the probability of formation of NBF obtained from solutions of R1 as a function of C_s [7, 30]. These experiments were carried out at $C_{el} = 0.8$ mol dm^{-3} NaCl, because this was the C_{el} where NBF formation first occurred in foam films formed from solution of the rhamnolipid mixture R2/R1 = 1.2 [29]. Our experiments showed that stable NBF (*i.e.*, with lifetime greater than 15 min) could form from R1 solutions with C_s higher than 3×10^{-4} mol dm^{-3}. The pH of these solutions was $\sim$5.8.

NaCl (Merck, suprapur) was used as an electrolyte. To remove eventual organic impurities it was roasted at 550°C for 2 h. Throughout the experiments, triple-distilled water was used (specific conductivity $\kappa = 1 \times 10^{-6}$ S cm^{-1}, pH $\sim$ 5.8).

Methods

The foam film with a radius r = 100 μm is formed by withdrawing the studied liquid from the biconcave drop hanging in the glass tube with a radius R = 2.4 mm of the Scheludko–Exerowa measuring cell (Figures 2a and 3) [1, 7, 30] that allows work at constant capillary pressure, P_σ. To avoid evaporation from the film, the bottom of the tightly closed cell is covered with a layer of the studied solution. Before each experiment the cell was cleaned with hot chromic mixture and thoroughly washed with triple-distilled water.

The measuring cell with a porous plate made of a fritted glass disk (Figure 2b), designed by Exerowa and Scheludko [7, 30, 33], was used for studies of foam films submitted to different external pressures. The foam film is formed in a hole with a radius of 500 μm drilled in the fritted glass plate that serves as a film holder. It is fused to a glass capillary whose free end is exposed to atmospheric pressure. When

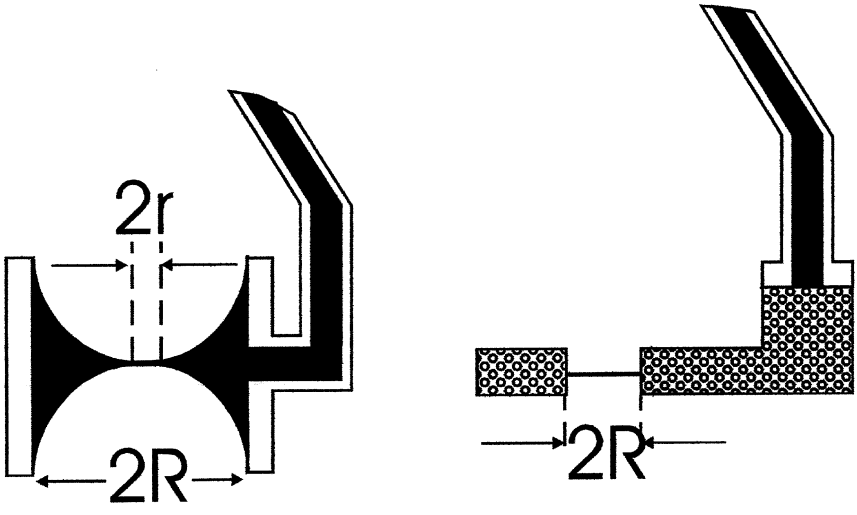

(a) (b)

FIGURE 2 (a) Scheludko–Exerowa cell for film thickness measurements at constant capillary pressure [1, 7]; R, radius of the cylindrical holder where the film is formed; r, radius of the foam film, (b) Exerowa–Scheludko porous plate cell [33]; R, radius of the hole drilled in the porous plate.

the film is formed in the closed gas-tight measuring cell the film meniscus penetrates into the pores of the film holder. The pore size determines the maximum capillary pressure, P_σ, that can be reached until the gas phase can enter them. The radii of the pores in the cell that we used were in the range of 16–40 μm. This allowed us to increase P_σ to about 1.5×10^3 Pa, considering that the surface tension of the solution was about 30 dynes/cm [34]. In this cell the film thickness changes in accordance with the applied external pressure, thus allowing the direct measuring of disjoining pressure (thickness) isotherms at equilibrium $P_\sigma = \Pi$, where Π is the disjoining pressure in the film.

Before each experiment this cell was thoroughly washed with water and then put in an oven where it was heated for several hours at 700°C. After that it was again washed with hot and cold triple-distilled water.

The thickness of the films was measured using the modernized microinterferometric method of Scheludko and Exerowa [1, 7, 30].

The schematic shown in Figure 3 illustrates the principle of this technique. The measuring cell is fixed in a thermostatting device joined to the stage of a reflected light microscope with suitably adapted optics that allows both visual observation and photometering.

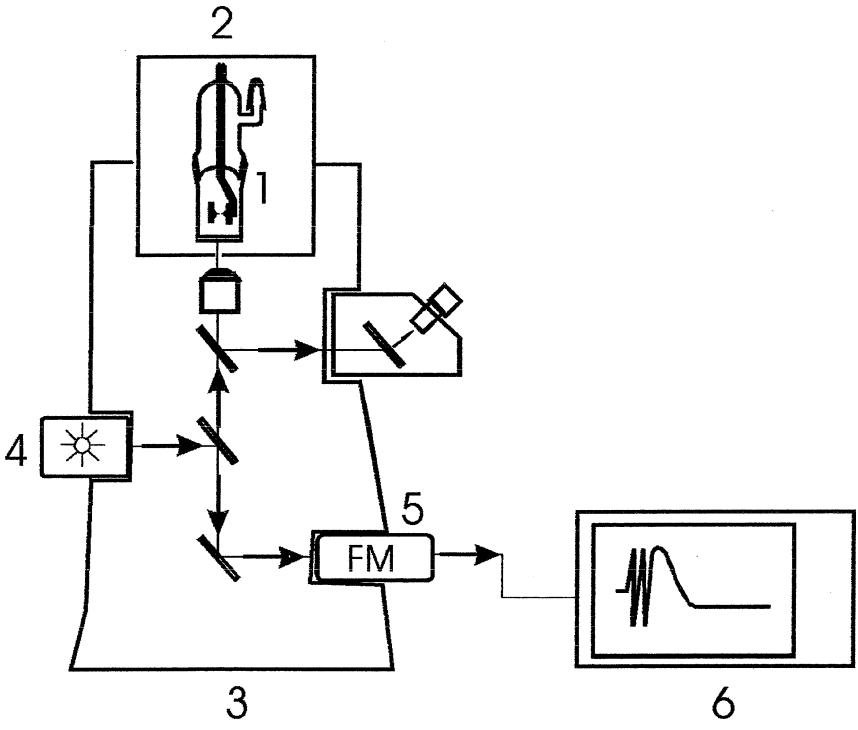

FIGURE 3 Schematic of the interferometric technique for film thickness measurements [1, 7]. 1, measuring cell; 2, thermostating device; 3, microscope; 4, halogen lamp; 5, photomultiplier; 6, recording device.

The apparatus is situated in a thermostatted room where precautions are taken to avoid vibrations.

The process of film thinning is recorded by a special electronic system registering the intensity of the monochromatic light with wavelength $\lambda = 546\,\text{nm}$ reflected from both film surfaces. During our measurement we assumed that the film had reached its equilibrium thickness when the intensity of the reflected light did not change for 5 min. To confirm that equilibrium thickness value, we waited for 5 min more and again checked the light intensity.

The thin liquid film–pressure balance technique [35] was used to measure directly the disjoining pressure isotherms ($\Pi(h)$). This technique allows gradual and reversible change of the pressure in the measuring cell with an accuracy $\pm 5\,\text{Pa}$.

Film thickness is calculated from the ratio between the measured intensities of the reflected monochromatic light, I, corresponding to

a certain thickness, and $I_{\max}$, corresponding to the interference maximum, according to the formula [1, 7]

$$h_w = \frac{\lambda}{2\pi n}\left(k\pi \pm \arcsin\sqrt{\frac{I/I_{max}}{1+[(n^2-1)/2n]^2(1-I/I_{max})}}\right), \qquad (1)$$

where k is the interference order and h_w is the so-called equivalent film thickness *i.e.*, the thickness of a foam film with refractive index of the solution, n, in our case $n = 1.333$.

In fact, the so-obtained equivalent film thickness, h_w, is slightly larger than the real film thickness, h, because the refractive index of the surfactant layers is higher than the refractive index of the solution from which the film is obtained. Thus, the "real" film thickness, h, is obtained using a five-layer model accounting for the film structure [36]:

$$h = h_w - 2h_1\left(\frac{n_1^2 - n^2}{n^2 - 1}\right) - 2h_{pg}\left(\frac{n_{pg}^2 - n^2}{n^2 - 1}\right), \qquad (2)$$

where h_1 and n_1 are the thickness and refractive index of the hydrophobic layers formed from the hydrocarbon tails of the absorbed molecules, and h_{pg} and n_{pg} denote the thickness and the refractive index of the polar head groups (Figure 4). The values of $h_1 = 1.1$ nm and h_{pg} = 0.42 nm were determined from the molecular models (Figure 1). The refractive index $n_1 = 1.397$ was approximated to that of octane. To determine n_{pg} we measured the refractive index of rhamnose solutions using an Abbé-type refractometer. We assumed that $n_{pg} = 1.386$,

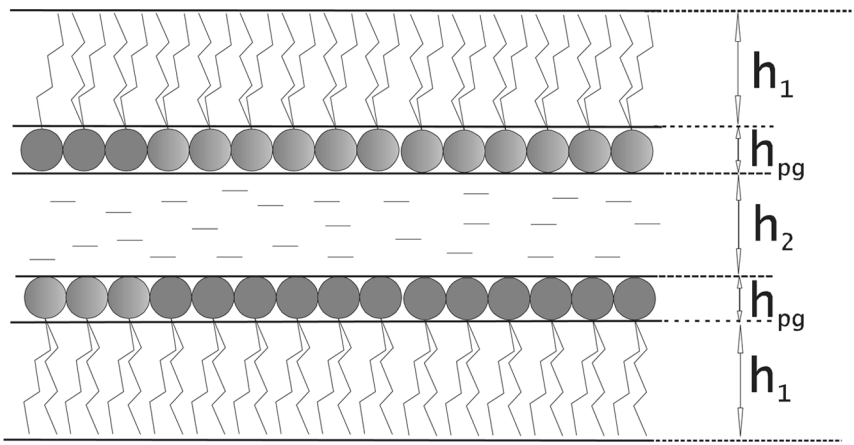

FIGURE 4 Foam film structure.

approximating it to the refractive index of a 60% rhamnose solution, as was suggested in previous studies of foam films stabilized with a sugar-based surfactant [37]. In this way we obtain $h = h_w - 0.7\,\text{nm}$. We should note that our measurements of the refractive index of rhamnose solutions showed that it increased from 1.371 to 1.386 in the concentration interval of 40–60%. The substitution of $n_{pg} = 1.386$ with the lowest measured value in Equation (2) leads to a change of only 0.1 nm in the obtained values of h.

Finally, the thickness h_2 of the aqueous core can be obtained by substracting the thickness of the surfactant layers from h:

$$h_2 = h - (2h_1 + 2h_{pg}), \tag{3}$$

The accuracy of thickness measurements with this microinterferometric technique is ± 0.2 nm.

All measurements were carried out at constant temperature T = 22°C.

EXPERIMENTAL RESULTS AND DISCUSSION

Figure 5 represents the real thickness $h = h_w - 0.7\,\text{nm}$ (Equation (2)) of rhamnolipid foam films as a function of the concentration of NaCl (C_{el}). As seen, increase in NaCl concentration leads to decrease in film thickness. In the C_{el} interval of $10^{-3}\,\text{mol dm}^{-3} - 3 \times 10^{-2}\,\text{mol dm}^{-3}$ NaCl, the thickness of the obtained films decreases from 67 to 21 nm. These films are CFs that look silver when observed in reflected white light. Black spots that expand and fill the whole film area are first observed at $C_{el} = 0.1\,\text{mol dm}^{-3}$ NaCl, where the films are 10.3 nm thick, so this C_{el} denotes the CF-to-CBF transition. The thickness of CBF decreases to about 4.8 nm with increase in C_{el} up to $0.8\,\text{mol dm}^{-3}$ NaCl. After that C_{el} the change of film thickness is within the experimental error, so we can consider that $C_{el} = 0.8\,\text{mol dm}^{-3}$ NaCl is the critical electrolyte concentration ($C_{el,\,cr}$) that indicates the formation of NBF [1, 7, 30].

The obtained $h(C_{el})$ curve agrees well with the $h(C_{el})$ dependence of the foam films formed from aqueous solutions of rhamnolipids R2/R1 = 1.2 (Figure 6). The calculation of h of the R2/R1 = 1.2 films was made according to Equation (2) considering the similarity in the structure of the R2 and R1 molecules [34]. So, the $h(C_{el})$ curve shows that, similar to the films formed from rhamnolipid mixtures, long-range DLVO forces are operative in CF and CBF formed from the R1 solutions. They lead to the decrease of h with the increase of C_{el} in accordance with the basic assumptions of the DLVO theory [2, 8].

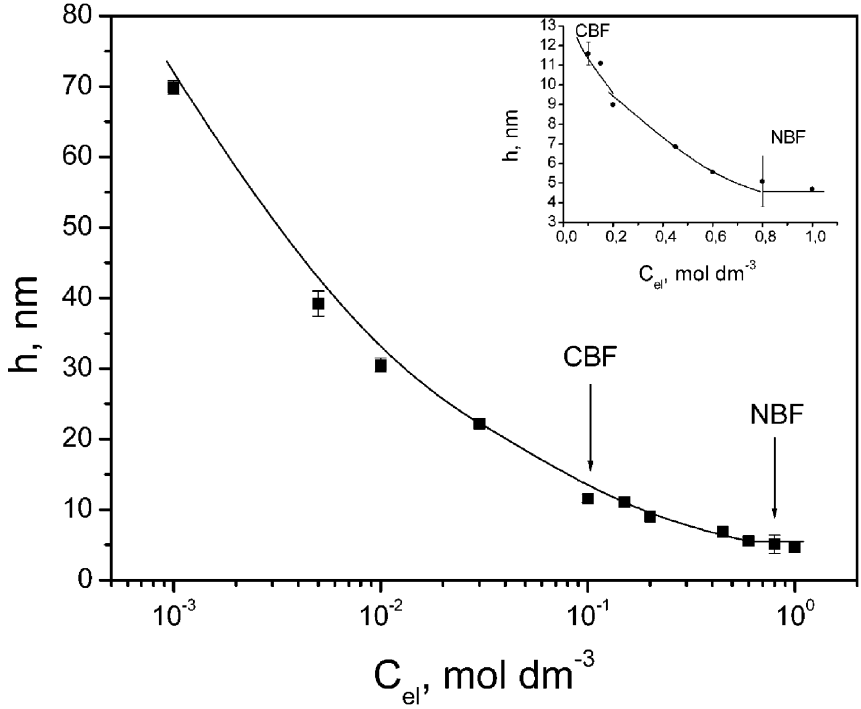

FIGURE 5 Real film thickness (h), of R1 foam films as a function of NaCl concentration (C_{el}): $C_s = 5 \times 10^{-4}$ mol dm^{-3}, r = 100 μm, $P_\sigma = 25$ Pa, and T = 22°C.

Also, in both cases the transitions CF to CBF and CBF to NBF are observed at the same C_{el}. Here, however, the C_s used in the case of the R1-stabilized films is higher than the previously used $C_s = 10^{-4}$ mol dm^{-3} R2/R1 = 1.2 [29]. The higher ionic strength of the R1 solutions resulting from the higher C_s leads to a lower film thickness at $C_{el} = 10^{-3}$ mol dm^{-3} NaCl, compared with that of the films formed from the mixed rhamnolipid solutions. The relative contribution of C_s to the ionic strength of the rhamnolipid solutions decreases with the increase of C_{el}, and the differences between the $h(C_{el})$ curves obtained with R1 foam films and R2/R1 = 1.2 foam films disappears at higher C_{el}.

The observed continuous transition to NBF is evidence of the action of additional non-DLVO repulsive forces, leading to an additional positive component of the disjoining pressure. The comparatively large scatter of h found at $C_{el} = 0.8$ mol dm^{-3} NaCl, clearly seen in the inset of Figure 5, however, distinguishes the R1 foam films from those

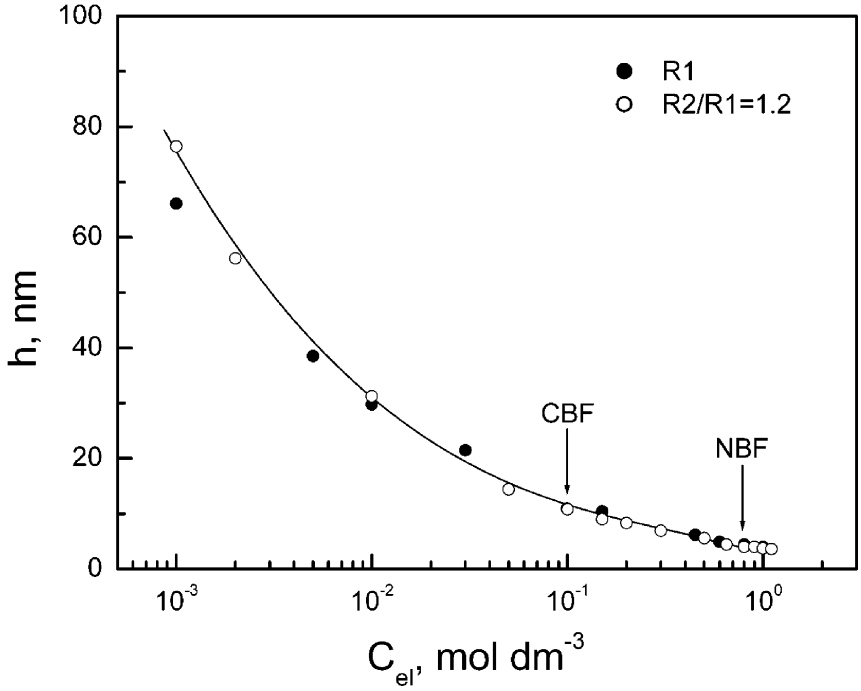

FIGURE 6 Real film thickness (h), of R1 ($C_s = 5 \times 10^{-4}\,\mathrm{mol\,dm^{-3}}$) and R2/R1 = 1.12 ($C_s = 10^{-4}\,\mathrm{mol\,dm^{-3}}$) foam films as a function of NaCl concentration (C_{el}): r = 100 μm, $P_\sigma = 25$ Pa, and T = 22°C.

stabilized with R2/R1 = 1.2. One possible reason for that effect can be found in the molecular aggregation in the R1 solutions. Studies of Ishigami *et al*. [38] show that rhamnolipids form aggregates whose reversible transformation from vesicles through lamellae, lipid particles, and micelles depends on the pH of the solutions. Our work was carried out at pH were conversion equilibria between vesicles and lamellae have been observed. It is possible that the observed experimental scatter evidences the changing morphology of molecular aggregates. The high C_{el} where these effects are observed could also lead to changes in the configuration of the molecules and ions in the adsorbed layers.

To get more information about the molecular interaction forces in the R1-stabilized films, we carried out direct measurements of the disjoining pressure isotherms at different electrolyte concentrations. Figure 7 shows the obtained $\Pi(h)$ curve for R1 foam films obtained at $C_{el} = 10^{-3}\,\mathrm{mol\,dm^{-3}}$ NaCl. The lowest value of $\Pi = P_\sigma = 25\,\mathrm{Pa}$ is that of the film formed in the cell used for the investigations at

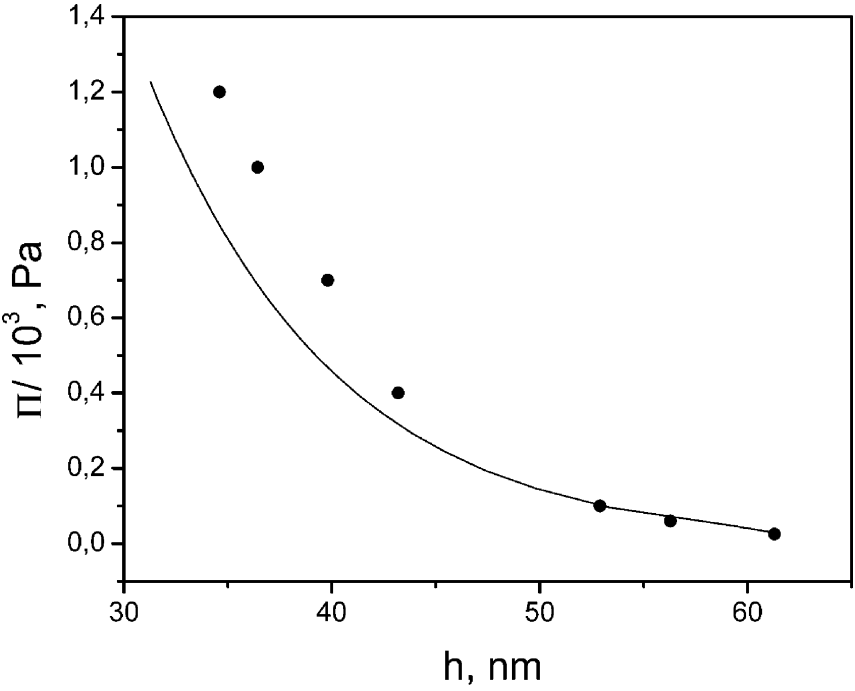

FIGURE 7 $\Pi(h)$ isotherm of foam films stabilized with R1. $C_s = 5 \times 10^{-4}$ mol dm^{-3} R1. $C_{el} = 10^{-3}$ mol dm^{-3} NaCl: Points, experiment; solid curve, theoretical results calculated according to the DLVO theory equations for $\varphi_o = 52$ mV an $\sigma_o = 5$ mC m^{-2}.

constant capillary pressure (Figure 2a). It was found using Laplace's equation $P_\sigma = 2\sigma/R$, where R is the radius of the capillary of the measuring cell where the film is formed, and $\sigma = 30$ mN m^{-1} [34] is the surface tension of the R1 aqueous solution. The increase of $\Pi = 25$ Pa to $\Pi = 1.2 \times 10^3$ Pa leads to decrease of the real film thickness, h, from 61 to 35 nm.

According to the basic equations of the classic DLVO theory, at equilibrium the disjoining pressure, Π, equals the sum of the repulsive electrostatic (Π_{el}) and attractive van der Waals (Π_{vw}) components of the disjoining pressure:

$$\Pi = \Pi_{el} + \Pi_{vw} = P_\sigma. \tag{4}$$

The comparison of the obtained experimental $\Pi(h)$ isotherm with the DLVO theoretical predictions was carried out by means of the computer program involving the solution of the complete

Poission–Boltzmann and Lifshitz equations for Π_{el} and Π_{vw} [35]. The computation of Π_{el} is based on the algorithm [39] that allows the assumption of both constant potential of the diffuse electric layer and constant surface charge density. The procedure [39] requires determining the distance, d, between the planes of origin of the diffuse electric layer potential, φ_0. We assumed that d equals the distance between the centres of the head groups of the adsorbed rhamnolipid, molecules [40]. Using the data for $h_1 = 1.1\,\text{nm}$ and $h_{pg} = 0.4\,\text{nm}$ (Figure 1), we found that $d = h - (2.2 + 0.4)\,\text{nm}$, h being the real film thickness (Equation (2)). C_{el} was determined as a sum of the concentrations of the rhamnolipid ions and the electrolyte added to the solutions. Following the data for $\text{pK}_\text{a} = 5.6$ found by Ishigami *et al*. for rhamnolipids of similar structure [38], we found that at $\text{pH} = 5.8$ about 60% of the rhamnolipid molecules are dissociated. Thus, for the films obtained from the R1 solutions of $C_\text{s} = 5 \times 10^{-4}\,\text{mol dm}^{-3}$ with $10^{-3}\,\text{mol dm}^{-3}$ NaCl added, $C_{el} = 1.3 \times 10^{-3}\,\text{mol dm}^{-3}$. Π_{vw} was assessed according to the equation of Donners *et al*. [41], allowing the numerical evaluation of the Lifshitz expressions for three-layers systems. According to this model the aqueous core of the rhamnolipid foam film comprises the rhamnolipid head groups, so its thickness equals $h - 2h_l$. Though the equation [41] has been derived for three-layer systems with slightly different parameters of the adsorbed layers, its use is justified because of the relatively small effect of these parameters on Π_{vw}, at least for thicknesses above 5 nm. So we derived the theoritical curve shown in Figure 7 computed at the conditions of a surface potential, φ_0, of 52 mV and corresponding surface charge density, σ_0, of $5\,\text{mC m}^{-2}$. It should be noted that in this case the computations carried out at the boundary conditions of constant potential, φ_0, or constant surface charge density, σ_0, yielded practically the same results for Π.

The obtained electrical parameters at the film interfaces seem rather low when compared with the respective values of φ_0 and σ_0 of foam films stabilized with other ionic surfactants [7, 14, 35, 42, 43]. They are, however, higher that φ_0 and σ_0 found for foam films formed from solutions of nonionic surfactants, including sugar-based ones at concentrations close to the critical micellar concentration (CMC) [17, 44, 45]. So the obtained φ_0 and σ_0 can be considered as evidence of the formation of a mixed adsorbed layer formed from R1 ions and neutral molecules. This is possible because the surfactant in the bulk is not completely dissociated, and neutral R1 molecules can adsorb at the film interfaces as well. Their surface concentration can reach high values due to the lack of elctrostatic repulsion between their hydrophilic head groups.

As seen in Figure 7, a deviation from the theoretical DLVO curve is found for $h < 40\,\text{nm}$. The obtained higher values compared with the DLVO predictions can be attributed to the action of additional non-DLVO repulsive forces in the R1 foam films. Possibly, these forces originate from the change of the molecular configuration of the surfactant in the film due to the above-discussed aggregation process.

In order to get more insight into the nature of these non-DLVO forces, we measured $\Pi(h)$ isotherms of CBF formed from R1 solutions of $C_{el} = 0.15\,\text{mol dm}^{-3}$ NaCl. Figure 8 shows the obtained curves from two separate experiments carried out on different days. Each isotherm was repeated twice to ensure the reproducibility of the experiment.

As seen in Figure 8, the starting points of both isotherms obtained in the Scheludko–Exerowa cell (Figure 2a) at a pressure of 25 Pa coincide at $h = 9.7\,\text{nm}$. An increase in pressure, however, leads in both cases to steplike film thinning. Although the effect seems rather irreproducible, when both measurements are compared we can see that the film thinning process follows the same trend. In curve 1 the initial

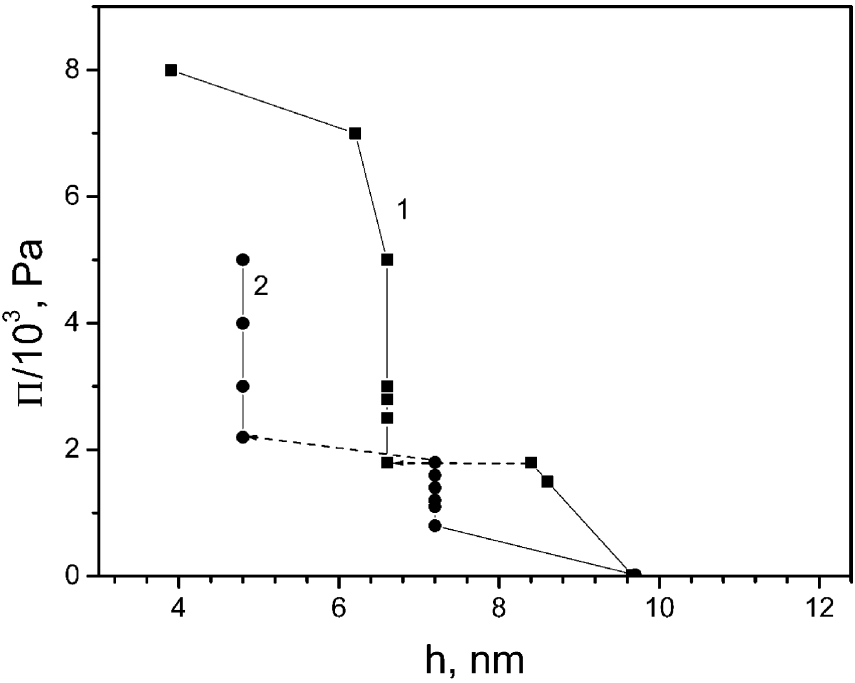

FIGURE 8 $\Pi(h)$ isotherm of common black foam films stabilized with R1 aqueous solutions. $C_s = 5 \times 10^{-4}\,\text{mol dm}^{-3}$ R1. $C_{el} = 0.15\,\text{mol dm}^{-3}$ NaCl, T = 22°C.

slight increase in pressure causes a decrease in h of 1.2 nm. After several minutes a discrete decrease of h of about 2 nm is observed. After that h remains practically constant with the increase in Π up to 7×10^3 Pa. At that pressure, however, another step to a thickness of 4 nm corresponding to the thickness of NBF is observed. Further increase of applied pressure leads to the rupture of the film. During the second experiment (curve 2) initial decrease of h with increase of the applied pressure is observed, followed by a range of constant h values and again to a steplike transition to films of $h = 4.8$ nm. Although this film ruptures at lower pressure than that observed in curve 1, the step in the curve occurs at the same Π.

Stepwise thinning (or stratification) of black films with one consecutive transition from one metastable state to another has been described in a number of studies starting with Johonnott [46] and Perrin [47]. Such a phenomenon has been observed in thin liquid films stabilized with various types of surfactants [14, 17, 48–53], including the specific case of a foam film from aqueous micellar solutions of surfactant mixtures containing an organic phase [53] and also in emulsion [54] and asymmetric gas/water/oil films [55]. In most cases, however, such thinning occurs spontaneously, under constant capillary pressure for horizontal films and gravitional field for the vertical films. Steplike decrease of h of foam films formed from aqueous solutions containing sodium dodecylsulphate at concentrations above the CMC with increase of the imposed pressure has been demonstrated by Bergeron and Radke [14]. In these studies, however, the stepwise decrease of film thickness occurred in the range of very low Π (40–60 Pa).

A discrete film thinning under the action of imposed capillary pressure is described in a previous study of microscopic horizontal foam films of the phospholipid fraction of lung surfactant formed from water–ethanol solutions [17]. Similar to the present case, irreproducibility of the pressure of film rupture and the corresponding h has been observed. It is speculated that this stepwise decrease of h is due to the existence of lamellar structures in the film. With the increase of the applied pressure, these structures are being ejected and films of lower thickness are obtained.

It is quite possible that the steplike $\Pi(h)$ isotherms evidence lamellar structures formed within the R1 films as well (Figure 9); moreover, the existence of lamellar rhamnolipid structures has been found and studied [38]. These $\Pi(h)$ isotherms distinguish the R1 films from those formed from the R2/R1 = 1.2 mixture [29], where the obtained $\Pi(h)$ isotherm at $C_{el} = 0.15\,\mathrm{mol\,dm^{-3}}$ displays a very slight decrease of h from 10 nm to 8 nm with increase of Π to pressures higher

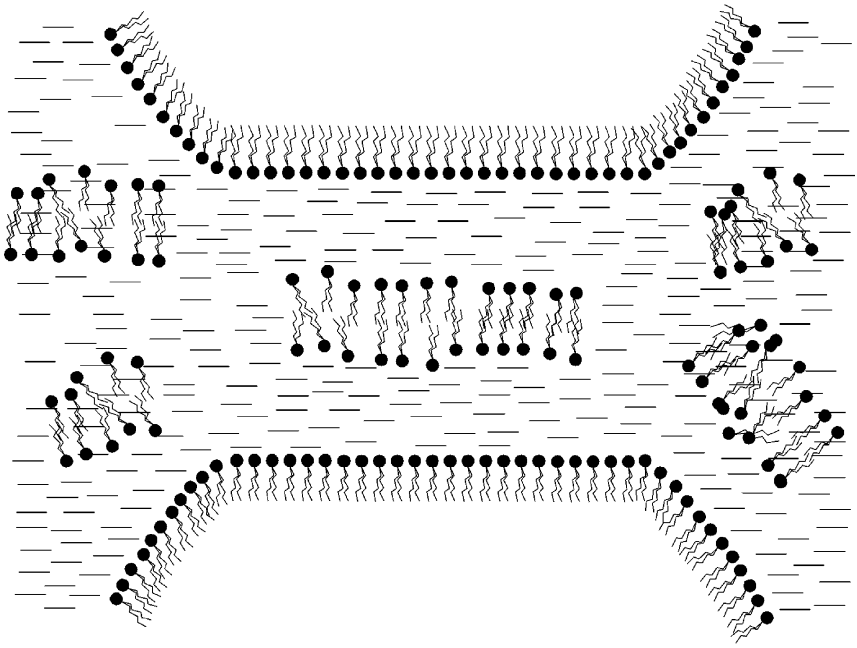

FIGURE 9 Lamellar structures formed in CBF of R1.

than 4×10^4 Pa. Besides, within the experimentally studied Π range the R2/R1 = 1.2 film did not rupture. Probably in that case the different saccharide head groups of the adsorbed rhamnolipids determine different organization and composition of the adsorbed layers. Additional evidence of such effects is the formation of stable NBF from 10^{-4} mol dm^{-3} R2/R1 = 1.2 solutions, while R1 solutions form stable NBF only above $C_s = 3 \times 10^{-4}$ mol dm^{-3} R1.

We also performed measurements of $\Pi(h)$ isotherms of foam films obtained at $C_{el} = 1$ mol dm^{-3} NaCl where NBFs are obtained. The results showed that the increase of the applied pressure to 1×10^3 Pa did not lead to any change of the film thickness, thus corroborating the bilayer structure of these films.

CONCLUDING REMARKS

The information obtained from the present studies of foam films formed from solutions of a single rhamnolipid contributes to the understanding of the nature of the surface forces in rhamnolipid foam films. The obtained results show that DLVO surface forces are

operative in CF and CBF. The comparison of experimental data with the DLVO theoretical predictions yields a potential of the diffuse electric layer of about 50 mV and a surface charge density of 5 mC m^{-2}. The deviations from the theoretical predictions, found for films thinner than 40 nm, are attributed to additional non-DLVO types of surface forces. The experimental $\Pi(h)$ isotherms obtained for the CBF show that, most probably, these additional surface forces result from an aggregation process, leading to the formation of lamellar structures in the foam film. This consideration is in accordance with previous studies of rhamnolipids [26] as well as with the recent studies [56] that evidence the formation of premicellar aggregates of fatty acids even at very low concentrations. According to Kanicky and Shah [56], at the pK_a where half of the fatty acid molecules are ionised the strong ion–dipole interaction between the adjacent carboxyl groups leads to the formation of ion–dipole-stabilized complexes (generally referred to as acid soaps). As our research was conducted at a pH where about 60% of the R1 molecules are ionized similar aggregation behavior is quite possible, although the concentration of R1 used in the present study is higher than the CMC [34]. In this respect it is expected that our future studies dealing with the effect of pH on the properties of rhamnolipid foam films will provide further and unambiguous information on the nature of surface forces operative in different types of rhamnolipid foam films.

REFERENCES

[1] Scheludko, A., *Adv. Colloid Interface Sci.* **1**, 391–464 (1967).
[2] Derjaguin, B. V., *Theory of Stability of Colloids and Thin Films* (Consultants Bureau, New York, 1989).
[3] Sonntag, H. and Strenge, K., In: *Koagulation und stabilität disperser Systeme* (VEB Deutscher Verlag der Wissenschaften, Berlin, 1970), Chap. 2.5, pp. 64–100.
[4] Mysels, K. J., Shinoda, K., and Frankel, S., *Soap Films* (Pergamon, New York, 1959).
[5] Clunk, J. S., Goodman, J. F., and Ingram, B. T., *Thin liquid films*, In: *Surface and Colloid Science*, Matijevic, E. (Ed.), (Wiley-Interscience, London-New-York, 1971), Vol. 3, pp. 167–239.
[6] Derjaguin, B. V., Churaev, N. V., and Muller, V. M., *Surface Forces* (Consultants Bureau, New York, 1988).
[7] Exerowa, D. and Kruglyakov, P., *Foam and Foam Films*, (Elsevier, Amsterdam, 1998), Chaps. 2, 3, pp. 42–343.
[8] Verwey, E. J. W. and Overbeek, J. Th. G., *Theory of Stability of Lyophobic Colloids* (Elsevier, Amsterdam, 1948).
[9] Israelaschvili, J., *Adv. Colloid Interface. Sci.* **16**, 31–47 (1982).
[10] Pashley, R. M. and Israelachvili, J. N., *J. Colloid Interface Sci.* **101**, 511–523 (1984).
[11] Israelaschvili, J. and Wennerström, H., *J. Phys. Chem.* **96**, 520–531 (1992).

[12] Parsegian, V. A. and Evans, E. A., *Curr. Opp. Coll. Int. Sci.* **1**, 53–60 (1996).
[13] Sedev, R. and Exerowa, D., *Adv. Colloid Interface Sci.* **83**, 111–136 (1999).
[14] Bergeron, V. C. and Radke, J., *Langmuir*, **8**, 3020–3026 (1992).
[15] Exerowa, D., Churaev, N. V., Kolarov, T., Esipova, N. E., Panchev, N., and Zorin, Z. M., *Adv. Colloid Interface Sci.* **104**, 1–24 (2003).
[16] Exerowa, D., Kolarov, T., Esipova, N. E., Yankov, R., and Zorin, Z. M., *Colloid J.* (*in English*), **63**, 1–8 (2001).
[17] Exerowa, D. and Lalchev, Z., *Langmuir* **2**, 668–671 (1986).
[18] Cohen, R., Exerowa, D., and Yamanaka, T., *Langmuir* **12**, 5419–5424 (1996).
[19] Yamanaka, T., Tano, T., Kamegaya, O., Exerowa, D., and Cohen, R. D. *Langmuir* **10**, 1871–1876 (1994).
[20] Exerowa, D., *Adv. Colloid Interface Sci.* **96**, 75–100 (2002).
[21] Rosenberg, E. and Ron, E. Z., *Appl. Microbiol. Biotechnol.* **52**, 154–162 (1999).
[22] Banat, I. M., Makkar, R. S., and Cameotra, S. S. *Appl. Microbiol. Biotechnol.* **53**, 495–508 (2000).
[23] Parra, J. L., Guinea, J. Manresa, M. A., Robert, M., Mercadé, M. E., Comelles, F., and Bosch, M. P., *JAOCS*, **66**, 141–145 (1989).
[24] Patel, R. M. and Desai, A. J., *J. Basic Microbiol.* **37**, 281–286 (1997).
[25] Lang, S. and Wullbrandt, D., *Appl. Microbiol. Biotechnol.* **51**, 22–32 (1999).
[26] Ishigami, Y., Gama, Y., Fumiyoshi, I., and Choi, Y. K., *Langmuir* **9**, 1634–1636 (1993).
[27] Ishigami, Y. and Suzuki, S., *Progr. Org. Coatings* **31**, 51–61 (1997).
[28] Abalos, A., Pinazo, A. A., Infante, M. R., Casals, M., García, F., and Manresa, A., *Langmuir*, **17**, 1367–1371 (2001).
[29] Cohen, R., Ozdemir, G., and Exerowa, D. *Colloid Surfaces B: Biointerfaces* **29**, 197–204 (2003).
[30] Exerowa, D., Kashchiev, D., and Platikanov, D., *Adv. Colloid Interface Sci.* **40**, 201–256 (1992).
[31] Lang, S. and Wagner, F., In: *Biosurfactants: Production, Properties and Application*, Kosaric, N. (Ed.) (Marcel Dekker, New York, 1993), *Surfactant Science Series*, Vol. 48, pp. 251–268.
[32] Syldatk, C., Lang, S., Wagner, F., Wray, V., and Witte, L., *Z. Naturforsch.* **40**, 51–60 (1985).
[33] Exerowa, D. and Scheludko, A., *Compt. Rend. Acad. Bul. Acad.* **24**, 47–50 (1971).
[34] Peker, S., Helvaci, Ş., and Ozdemir, G., *Langmuir* **19**, 5838–5845 (2003).
[35] Exerowa, D., Kolarov, T., and Khristov, Khr., *Colloids Surfaces* **22**, 171–185 (1987).
[36] Duyvis, M., Ph.D. "The equilibrium thickness of free liquid films", Utrecht University, Utrecht, (1962).
[37] Persson, C. M., Claesson, P. M., and Johansson, I., *Langmuir*, **16**, 10227–10235 (2000).
[38] Ishigami, Y., Gama, Y., Nahahora, H., Yamaguchi, M., Nakahara, H., and Kamata, T., *Chem. Lett.* 763–766, (1987).
[39] Chan, D. Y. C., Pashley, R. M., and White, L. R., *J. Colloid Interface Sci.* **77**, 283–285 (1980).
[40] Cohen, R., Exerowa, D., Kolarov, T., Yamanaka, T., and Tano, T. *Langmuir* **13**, 3172–3176 (1997).
[41] Donners, W. A. B., Rrijnbout, J. B., and Vrij, A. J., *Colloid Interface Sci.* **60**, 544–547 (1997).
[42] Joosten, J. G. H., *Ber. Bunsenges. Phys. Chem.* **88**, 1153–1161 (1984).
[43] Bergeron, V., *Langmuir* **13**, 3474–3482 (1997).
[44] Kolarov, T., Cohen, R., and Exerowa, D., *Colloids Surfaces* **42**, 49–57 (1989).
[45] Stubenrauch, C., Schlarmann, J., and Strey, R., *PCCP* **4**, 4504–4513 (2002).

[46] Johonnott, E. S., *Philos. Mag*. **11**, 746–749 (1906).
[47] Perrin, J., *Ann. Phys*. (Paris) **10**, 160–164 (1918).
[48] Bruil, H. and Lyklema, H., *J. Nature (London), Phys. Sci*. **233**, 19–20 (1971).
[49] Balmbra, R. R., Clunie J. S., Goodman J. F., and Ingram B. T., *J. Colloid Interface Sci*. **42**, 226–231 (1973).
[50] Keuskamp, J. W. and Lyklema, J., In: *Adsorption at Interfaces*, Mittal, K. L., Ed. (American Chemical Society, Washington DC, 1975), *ACS Symposium Series 8*, pp. 191–193.
[51] Nikolov, A. and Wasan, D., *J. Colloid Interface Sci*., **133**, 1–12 (1989).
[52] Manev, E., Sazdanova, S., Rao, A., and Wasan, D., *J. Disp. Sci. Technol*. **3**, 435–463 (1982).
[53] Khristov, Khr., Exerowa, D., and Kruglyakov, P. M. *Colloids Surfaces* **78**, 221–227 (1993).
[54] Manev, E., Sazdanova, S., and Wasan, D., *J. Disp. Sci. Technol*. **5**, 111–117 (1984).
[55] Lobo, L. and Wasan, D., *Langmuir* **9**, 1668–1677 (1993).
[56] Kanicky, J. R. and Shah, D. O., *Langmuir* **19**, 2034–2038 (2003).